Journal of Applied Mechanics and Technical Physics, Vol. 42, No. 3, pp. 475–481, 2001

FLOW DYNAMICS OF AN INTENSIVELY EVAPORATING WAVE FILM OF A LIQUID

A. N. Pavlenko, V. V. Lel',
A. F. Serov, and A. D. Nazarov

UDC 536.24

Experimental results on the behavior of a laminar-wave film of liquid nitrogen evaporating intensively under conditions of a gravitational flow on a locally heated vertical surface are described. It was found that certain heat fluxes change significantly the shape of the residual layer and increase the relative amplitude of large waves. For the first time, data are obtained on the change in the probability density of the local film thickness as a function of the heat-flux density within the range of Reynolds numbers from 32 *to* 103*. The effect of the heat-flux density on the phase velocity and shape of large waves is shown. Heat-flux densities at which "dry" spots arise were determined as functions of the streamwise coordinate of the wave film of the saturated liquid.*

For intensification of heat- and mass-transfer processes, liquid film flows along the elements of the heat-exchanger surface are widely used. A great number of theoretical and experimental investigations on hydrodynamics of the wave flow of the evaporating liquid film have been performed [1–3]. Most papers deal with the film flow on test sections of large length, with water, water–glycerin mixture, and oils used as working liquids. Owing to this, the flow regimes of the evaporating film in experimental investigations were restricted by low heat-flux densities.

Nakoryakov and Schreiber [4] derived an equation describing the film flow at Reynolds numbers $\mathrm{Re} \gg 1$ for the case of heat-flux absence. The model proposed has no dissipative terms. As a consequence, this equation has no steady solutions in the form of finite-amplitude waves. It was shown [5] that dissipation arises in the next approximation in the small parameter. It follows from the analysis of this equation that the term related to surface tension is always negative, which leads to dissipation (damping of perturbations), and the term related to viscosity is positive, which leads to the growth of perturbations and energy transfer from the main stream to the perturbation. A real film flow is even more complicated. Application of statistical methods of data processing on the wave characteristics allowed us to determine the dependence between individual parameters.

Lyu and Mudawar [6] studied the dynamics of evaporating turbulence-wave films of water for Reynolds numbers at the upper point of the heated surface $\mathrm{Re}_+ > 3000$, using statistical methods. At the same time, the authors are not aware of any experimental investigations of the flow dynamics of the intensively evaporating laminar-wave films of a saturated liquid.

The stability of a waveless flow of the evaporating film down the vertical plane was investigated in [7, 8]. It is shown that evaporation exerts a destabilizing effect and expands the range of long-wave perturbations increasing in time. In [9], an integral approach was developed to describe the wave behavior on the evaporating film of a saturated liquid without assumption of the amplitude smallness. Trifonov described theoretically the emergence of "dry" spots on the heat-release surface by analyzing nonlinear regimes for different wave types in the low-Reynolds-number domain, where boiling in the evaporating liquid film is suppressed. It was shown theoretically [10] that the heat-transfer intensity is affected by three factors: heat conduction through the residual layer, heat conduction through the crests of large waves, and possible vortices inside the wave crests.

Kutateladze Institute of Thermal Physics, Siberian Division, Russian Academy of Sciences, Novosibirsk 630090. Translated from Prikladnaya Mekhanika i Tekhnicheskaya Fizika, Vol. 42, No. 3, pp. 107–115, May–June, 2001. Original article submitted July 10, 2000; revision submitted December 21, 2000.

0021-8944/01/4203-0475 $25.00

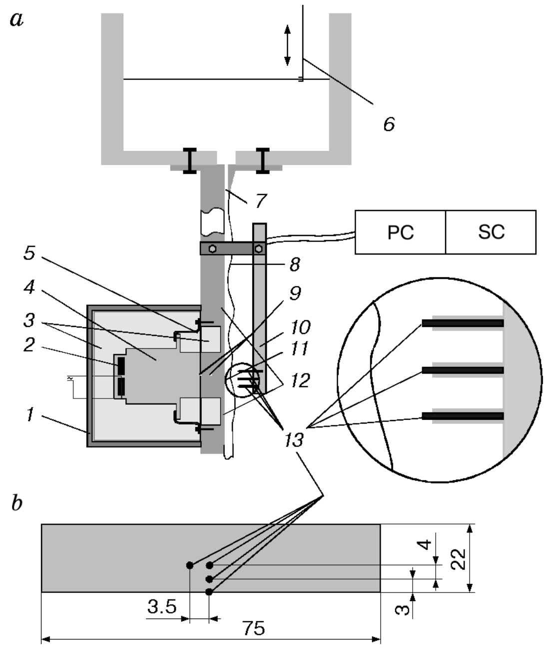

Fig. 1. Scheme of the test section (a) and front view of the heater (b): 1) protecting glass-cloth-laminate cover; 2) resistive heaters; 3) heat insulator; 4) copper heat conductor; 5) clamping plates; 6) travelling bar with level gauges; 7) distribution slot; 8) liquid nitrogen film; 9) thermistors; 10) microprobe board; 11) heat-release surface; 12) duralumin plate; 13) four capacitance micro probes; PC is the primary converter and SC is the secondary converter.

Since the height of packet stacks of plate facilities in cryogenic engineering is not large, and viscosity, surface tension, and limiting wetting angle of cryogenic liquids are small, the use of approximate dependences available in the literature for calculation of characteristics of the evaporating wave film of a cryogenic liquid should be supplemented by experimental data. However, in order to obtain the data, one has to perform some investigations in the range of cryogenic temperatures, which is very difficult to do.

The objective of the present work is to study experimentally the flow dynamics of an intensively evaporating laminar-wave liquid film flowing down a vertical heated surface.

Experimental Facility. The scheme of the test section, where the experiments were performed, is presented in Fig. 1. A detailed description of the experimental facility can be found in [11]. The experiments were performed at atmospheric pressure with nitrogen used as a working liquid. Heat exchange occurred during surface evaporation of the liquid film heated at the inlet up to the saturation temperature. The Prandtl number under the given conditions for liquid nitrogen is $\mathrm{Pr} = 2.3$. The liquid nitrogen film from a slotted distributor flowed down the vertical surface of a (280×75)-mm duralumin plate 12 and fell onto the heat-release part of the surface. The distance from the slot to the region of local heating equal to 160 mm provided a liquid film flow along the heat-release surface in the regime of hydrodynamic stabilization. In the experimental process, the local film thickness was measured using a three-channel capacitance microprobe. A volumetric method was applied to register the liquid flow rate. The surface temperature (with thermistors) and the heat-flux density were measured. Fixation of the liquid level above the distribution slot provided a constant flow rate. The use of a calibrated vessel allowed us to control the liquid flow rate with a 4% error. Local heating was performed by resistive heaters from a stabilized source of current. The heat-flux density varied from 0 to $4 \cdot 10^4$ W/m^2 during the experiment and was measured with an error of about 5% (taking into account heat losses).

The heat flux passed to the plate through a copper heat conductor 4 in which twenty-four heaters 2 were installed (Fig. 1). The holding clamps 5 ensured the necessary contact of the copper heat conductor 4 and the plate. To reduce to minimum the heat flux from the heat-release region, some grooves were made with a 0.6 mm plate thickness at the bottom. The copper conductor was thermally insulated by a polyurethane insert 3 with a fixing glass-cloth-laminate cover 1. Three local temperature thermistors 9 of the PPT type, whose temperature calibration was performed within the range of 70–150 K, were mounted on the heated part of the plate. To provide the maximum close contact of the heat sensors and the heat-transferring wall and reduce heat losses to minimum through the output of the wire sensors, the holes in which the latter were installed were filled by copper powder. The heat-release-surface temperature was reconstructed from the data of thermal-sensor measurements by the heat-wall technique.

Four capacitance microprobes 13 that composed a block located opposite the heated region 11 (Fig. 1) along the film-flow direction were used to study the change in the local thickness of the liquid film and wave characteristics along the flow direction. The advantage of the variable capacitance method is that the microprobes used do not disturb the liquid flow and have a high sensitivity. The method is based on the principle of registration of the electrical capacitance of the gauge capacitor, depending on the thickness of the liquid film flowing down between its plates.

A high-frequency electrical signal proportional to the local liquid-film thickness is formed by the primary converter, which contains two identical self-excited generators working at a frequency of approximately 30 MHz. The oscillatory circuit of one of the generators contains a variable capacitance probe placed above the heat-exchanger surface. The amplitude of the output signal of the primary converter has a low-frequency component equal to the difference in generator frequencies (the beat frequency is about 100 kHz) and proportional to the film thickness under the probe. Subsequent processing of the signal is performed in the secondary converter, where the signal is detected, filtered, and amplified. A special module is used to measure the instantaneous frequency $f(\tau)$. Together with the service program, the module allows measurement of the beat frequency $f(\tau)$ in the minimum time $\tau = 0.5$ msec, which corresponds to the clock frequency of the film-thickness meter $F = 2$ kHz. The RAM memory for three simultaneously registered channels at the available clock frequency makes it possible to study the wave process on the film surface with the maximum frequencies up to 700 Hz. It is possible to set the optimum parameters of the registering equipment depending on the research tasks. In the present work, the film-flow regimes examined are characterized by frequencies up to 200 Hz. Therefore, the sampling interval of the measured frequency $f(\tau)$ is accepted equal to 1 msec. In this case, the sampling clock frequency is $F = 1$ kHz, which allows us to study the wave processes on the film surface within the frequency region up to 300 Hz with an error of frequency determination $f(\tau)$ less than 10^{-3}.

The local liquid-film thickness was calculated using the dependences of the probe capacity on the nitrogen film thickness $C(\delta)$ and the generator frequency on the probe capacity $f(C)$, which were used in a common program. The accuracy of transition from the function $f(\tau)$ to the function $\delta(\tau)$ was tested experimentally. For the chosen probe sizes, the error of the film-thickness measurement was ± 2.5 μm. The modified measurement method was described in more detail in [12].

Experimental Results. The film profile was measured at three points simultaneously in the flow direction at distances $x_1 = 15$ mm, $x_2 = 19$ mm, and $x_3 = 22$ mm from the upper edge of the heated region. For $\mathrm{Re}_+ = 38$, the values $x_1/\langle\lambda\rangle \approx 1.6$, $x_2/\langle\lambda\rangle \approx 2.0$, and $x_3/\langle\lambda\rangle \approx 2.3$ correspond to these distances ($\langle\lambda\rangle$ is the average wavelength). Such a scheme of the gauges allows obtaining information on variation of the flow character and the wave form under intensive evaporation of the liquid.

Figure 2 shows the characteristic profiles of the liquid-film thickness at the point x_3 for different heat-flux densities. When there is no heat release, the wave structure of the film is a periodical sequence of solitons divided by an extended residual layer of a roughly constant thickness (curve 1 in Fig. 2). The small capillary waves are clearly seen in the residual layer. It follows from the data analysis that, for low heat-flux densities $q/q_* \leqslant 0.6$ (q_* is the heat-flux density at which "dry" spots stable in time arise), the liquid-wave film thickness decreases due to evaporation of the residual layer without changing the wave form. Evaporation is responsible only for a small change in the mean film thickness and the residual layer of the liquid. As the heat-flux density increases up to values close to the value corresponding to the moment of formation of unstable local "dry" spots, a significant change in the wave amplitude and form is observed. It follows from Fig. 2 that, at high heat-flux densities ($q = 9.9 \cdot 10^3$ and $1.2 \cdot 10^4$ W/m^2), a significant nonuniform decrease in the residual layer thickness occurs in the period between two large waves. The minimum thickness of the residual layer of the liquid is reached at the time before the next incoming front of a large wave. In the heat-load range examined, the local Reynolds number $\mathrm{Re}_l = \mathrm{Re}_+ - 4qx_n/(\rho r)$ (ρ is the liquid density and r is the heat of evaporation) significantly changes over the scale of several characteristic wavelengths due to intensive evaporation. As the simplest heat-balance calculation shows, for the maximum heat-flux density, the local Reynolds number Re_l changes from 103 to 68 when the liquid film passes above the heating region up to the measurement point.

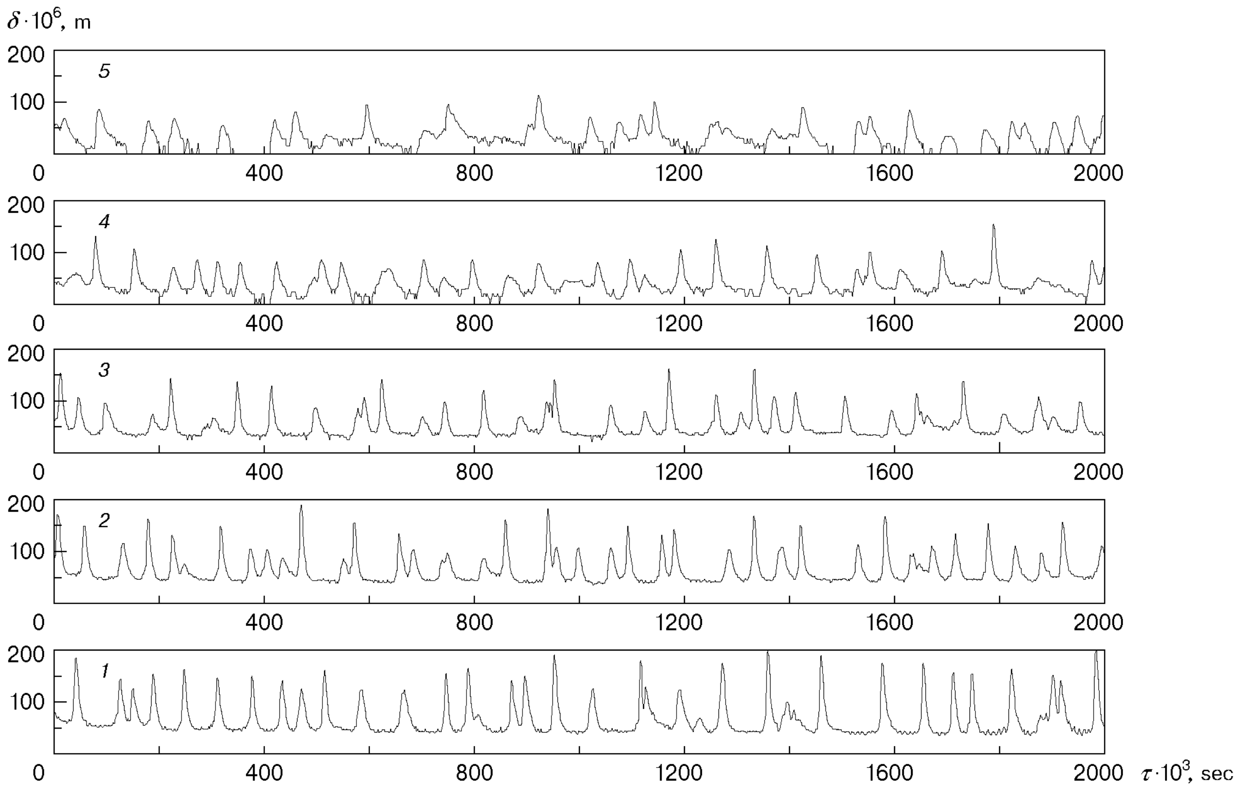

Fig. 2. Instantaneous thickness [$x_3 = 22$ mm ($x_3/\langle\lambda\rangle \approx 1.3$) and $\mathrm{Re}_+ = 103$] of the liquid-nitrogen film in a film flow along a vertical heat-release surface: 1) $q = 0$, $\langle\delta\rangle = 65.8 \cdot 10^{-6}$ m, $\delta_{\min} = 51.4 \cdot 10^{-6}$ m, and $\mathrm{Re}_l = 103$; 2) $q = 6.2 \cdot 10^3$ W/m^2, $\langle\delta\rangle = 65.0 \cdot 10^{-6}$ m, and $\mathrm{Re}_l = 85$; 3) $q = 7.8 \cdot 10^3$ W/m^2, $\langle\delta\rangle = 50.9 \cdot 10^{-6}$ m, and $\mathrm{Re}_l = 80$; 4) $q = 9.9 \cdot 10^3$ W/m^2, $\langle\delta\rangle = 39.1 \cdot 10^{-6}$ m, and $\mathrm{Re}_l = 74$; 5) $q = 1.2 \cdot 10^4$ W/m^2, $\langle\delta\rangle = 28.6 \cdot 10^{-6}$ m, and $\mathrm{Re}_l = 68$.

Figure 3 shows the probability density of the liquid-film thickness p versus the film thickness δ at the points $x_1 = 15$ mm ($\mathrm{Re}_+ = 38$) and $x_3 = 22$ mm ($\mathrm{Re}_+ = 51$) for different heat-flux densities. The probability density was calculated using statistical processing of the experimental data with a step from 3 to 5 μm. As the heat flux increases, the curve $p(\delta)$ in the region of small q is shifted to the left without significant changes if its form. When the heat-flux density approaches the critical values, the curve $p(\delta)$ becomes more gentle. The point corresponding to the maximum of the function $p(\delta)$ is shifted to the region of thinner liquid films. With increasing q, the probability of existence of a liquid film with a very small thickness increases. The reason for the finite value of the function $p(\delta)$ for $\delta = 0$ for high heat-flux densities is the beginning of the formation of local "dry" spots unstable in time. A further increase in q leads to the formation of "dry" spots stable in time on the heat-release surface; the probability density of the liquid-film thickness is described by the delta function. The onset conditions for these critical regimes in the above-mentioned range of Reynolds numbers were studied in detail in [11].

It is seen from Figs. 2 and 3 that the relative wave amplitude $A = (\delta_{\max} - \delta_{\min})/\delta_{\min}$ ($\delta_{\max}$ is the film thickness in the wave peak and $\delta_{\min}$ is the minimum thickness of the residual layer) as the heat-flux density q/q_* increases from 0.6 to 1. The increase in the relative wave amplitude in the process of instability development in the flow of an intensively evaporating film of a saturated liquid along the heated vertical surface, which was theoretically predicted in [9], was detected experimentally in the present work. The calculations were performed for the conditions $T = \mathrm{const}$ (T is the temperature of the heat-release surface) in the laminar-wave liquid flow ($\mathrm{Re}_+ = 20$) under conditions of a slowly changing solution, i.e., the approximation of a weak change in the current Reynolds number on the length scale of large waves was used in the calculations. The calculated forms of the wave surface of the evaporating liquid film corresponding to temperature differences $\Delta T = 0.23$ and 2.3 K for liquid nitrogen (ΔT is the temperature difference of the heat-release surface and liquid saturation at a given pressure) are also presented in [9]. The analysis of the above experimental results and calculations performed in [9] yields in identical location of the point of the most probable decrease in the liquid-film thickness and the formation of

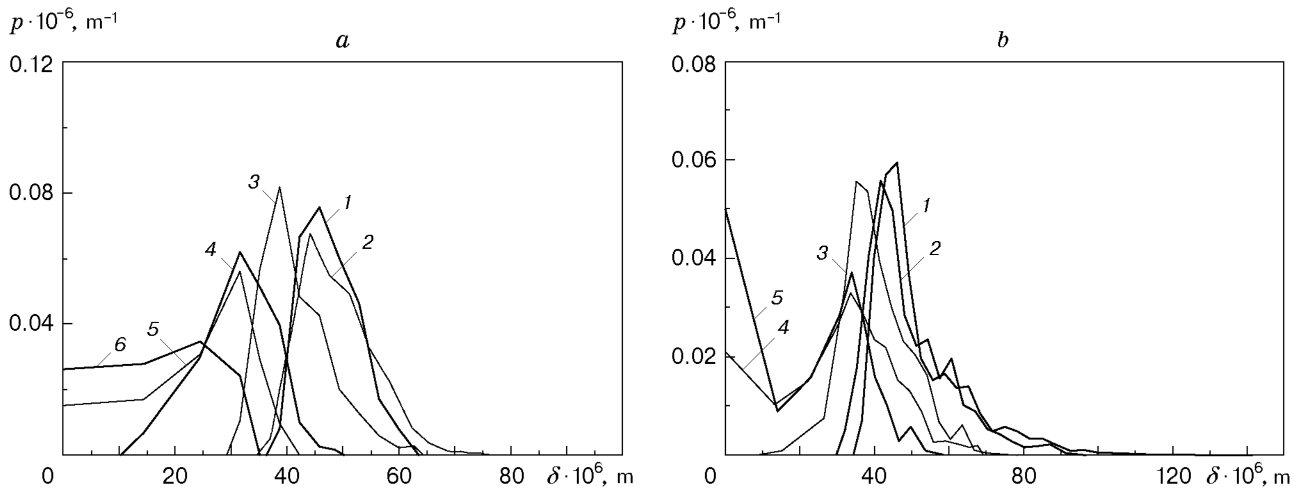

Fig. 3. Probability density of the liquid-film thickness for different heat-flux densities: (a) $x_1 = 15$ mm ($x_1/\langle\lambda\rangle \approx 1.6$), $\mathrm{Re}_+ = 38$, and $q = 0$ (1), $2.4 \cdot 10^3$ (2), $3.9 \cdot 10^3$ (3), $5.4 \cdot 10^3$ (4), $6.7 \cdot 10^3$ (5), and $8.2 \cdot 10^3$ W/m^2 (6); (b) $x_3 = 22$ mm ($x_3/\langle\lambda\rangle \approx 2.0$), $\mathrm{Re}_+ = 51$, and $q = 0$ (1), $3.3\cdot 10^3$ (2), $4.8\cdot 10^3$ (3), $6.8\cdot 10^3$ (4), and $9.5\cdot 10^3$ W/m^2 (5).

"dry" spots in the region immediately before the next front of the large wave. In the tests performed, a dependence close to linear of the residual layer thickness on time in the period between passing of the neighboring large waves is observed. It is seen from the theoretical analysis of instability of the intensively evaporating liquid film [9] that this dependence is significantly more nonlinear with a fast decrease in the thickness of the local liquid film in time just before the front of incoming large waves.

Figures 4–6 show the measurement results of the phase velocity of large waves. The experimental results obtained under adiabatic conditions are shown in Fig. 4. The phase velocity of large waves c, related to the characteristic velocity $V = g\delta_{\min}^2/(3\nu)$, is presented in the form of a dependence on the relative amplitude of large waves (g is the acceleration of gravity and ν is the kinematic viscosity). The scatter of experimental data is caused by the large measurement error of a very small thickness of the residual layer. Curve 1 in Fig. 4 corresponds to the calculations by the theoretical dependence

$$c = \frac{g\delta_{\min}^2}{\nu}\,(1 + A) \tag{1}$$

obtained in [3] for weak nonlinear forward-facing steps; curve 2 is constructed by the formula

$$c = \frac{g\delta_{\min}^2}{3\nu}\,(3 + 2.324A) \tag{2}$$

proposed in [13] for a sequence of solitons with a smooth residual layer between them at $\mathrm{Re} \approx 1$, $c/V \ll 1$, and $A \ll 1$. Curve 3 corresponds to a similar dependence from [14] for a sequence of solitons. It follows from Fig. 4 that the experimental data obtained for the phase velocity for natural waves under adiabatic conditions are also in satisfactory agreement with the theoretical curves in the region $A > 1$.

Intensive evaporation influences both the form of the wave surface and the phase velocity of large waves (Fig. 5). The phase velocity was determined by registration of the time of wave passing between the microprobes at the measurement points x_2 and x_3. It is seen from Fig. 5 that the average phase velocity of large waves decreases significantly with increasing heat-flux density. The most appreciable change in the phase velocity of large waves is observed in the region of high heat-flux densities, where the residual layer of the liquid film becomes significantly thinner, and local "dry" spots unstable in time arise.

Figure 6 shows the experimental dependences of the phase velocity of large waves on the amplitude for different heat-flux densities. With decreasing $\delta_{\max}$, the phase velocity of large waves also decreases during intensive evaporation. In regimes with the formation of local unstable "dry" spots with the greatest heat flux-density (points 5 in Fig. 6), a sharper change in the phase velocity is observed. Under these conditions, large waves propagate is over a nonwetted surface. A sharp deceleration of wave-crest propagation is apparently explained by the additional effect of the recoil reaction forces of vapor during intensive evaporation of the liquid film in the meniscus region.

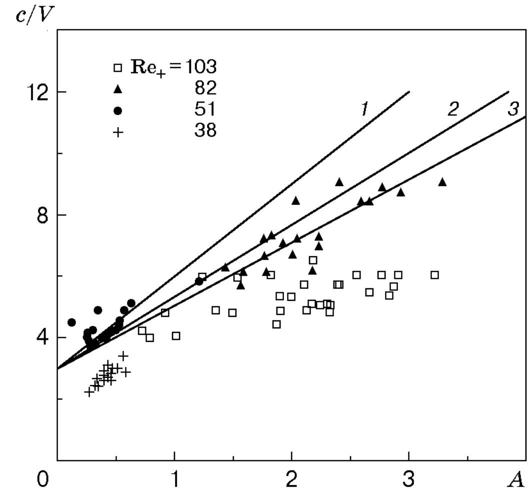

Fig. 4

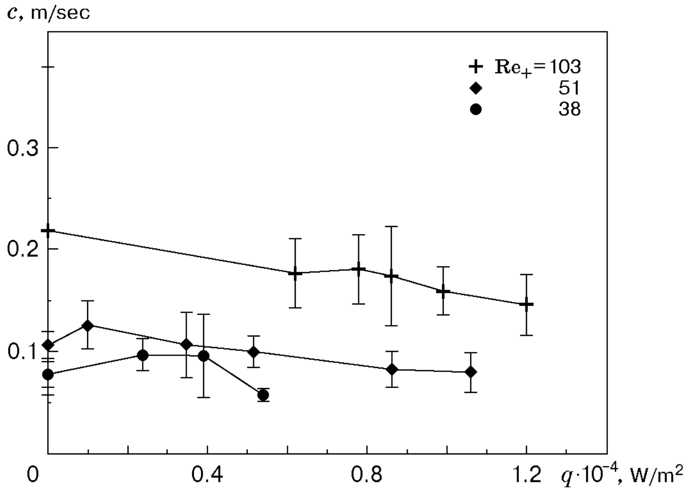

Fig. 5

Fig. 4. Dimensionless phase velocity of large waves c/V versus the relative amplitude A for $q = 0$: the solid curves refer to calculations of [3] (1), [13] (2), and [14] (3); the points are the experimental data.

Fig. 5. Dependence of the average phase velocity on the heat-flux density for different Reynolds numbers.

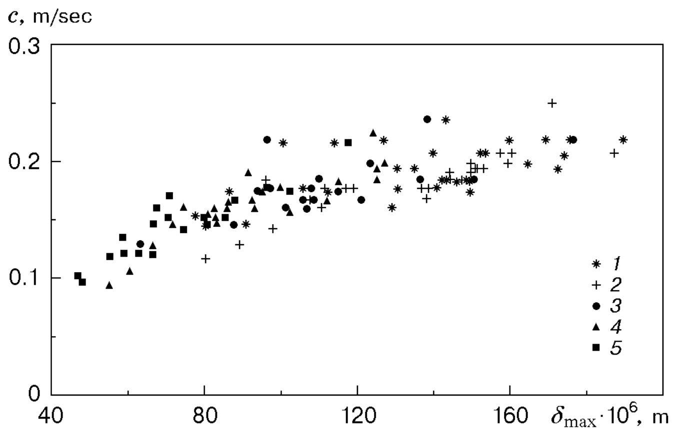

Fig. 6. Dependence of the phase velocity of large waves on the absolute amplitude for $\mathrm{Re}_+ = 103$ and $q = 0$ (1), $0.62 \cdot 10^4$ (2), $0.78 \cdot 10^4$ (3), 0.86×10^4 (4), and $1.2 \cdot 10^4$ W/m^2 (5).

When the values of the heat-flux density q_* reach their threshold, stable (nondisappearing) "dry" spots are formed. Stationary rollers are formed in front of the "dry" sports in the incoming liquid. In the region of low Reynolds numbers ($\mathrm{Re}_+ < 60$–80), the increase in time of "dry" spots at $q = q_*$ may lead to complete dehydration of the heat-release surface.

Conclusions. For the first time, with the use of a procedure of measurement of the local thickness of the liquid film, the dynamics of laminar-wave flow of an intensively evaporating saturated liquid film on a vertical heated surface was investigated. In the heat-exchange regimes studied, the average thickness of the liquid film changes considerably on streamwise linear scales comparable with the characteristic length of large waves.

The studies performed allow the following conclusions.

In the region of low heat-flux densities, the wave-film thickness decreases uniformly without significant changes in the wave form. In the range of large heat fluxes, a nonuniform decrease in the residual layers thickness on mean free paths comparable with the characteristic wavelength and a fast increase in the relative wave amplitude are observed. Therefore, the form of the probability-density distribution of the film thickness changes considerably.

The emergence of local zones in the residual liquid layer with a very fine film intensifies heat exchange in subcritical regimes, in which the development of local flows in crests of large waves seem to be observed. These effects should be taken into account for construction of numerical models of heat exchange in intensively evaporating wave liquid films.

The instability arising in the intensively evaporating residual layer when the threshold heat-flux densities leads to the formation of "dry" spots.

The experimental data on the phase velocity of natural large waves under adiabatic conditions satisfy the known dependences for a sequence of stationary solitons.

A more significant decrease in the phase velocity of large waves with increasing heat-flux density is observed in regimes with the formation of unstable "dry" spots.

The results obtained are of great importance for studying the dependence between the wave characteristics and local heat exchange, conditions of increasing "dry" spots, and development of crisis regimes in intensively evaporating laminar wave-liquid films.

The work was supported by the Russian Foundation for Fundamental Research (Grant No 00-02-17923).

REFERENCES

1. E. G. Vorontsov and Yu. M. Tananaiko, *Heat Exchange in Liquid Films* [in Russian], Tekhnika, Kiev (1972).
2. G. Gimbutis, *Heat Exchange in Gravitation Liquid Film Flow* [in Russian], Mokslas, Vilnus (1988).
3. S. V. Alekseenko, V. E. Nakoryakov, and B. G. Pokusaev, *Wave Flow of the Liquid Films*, Begell House, New York (1994).
4. V. E. Nakoryakov and I. R. Schreiber, "Waves on the surface of a thin layer of a viscous liquid," *Prikl. Mekh. Tekh. Fiz.*, No. 2, 109–113 (1973).
5. T. Prokopiou, M. Cheng, and H. C. Chang, "Long waves on inclined films at high Reynolds number," *J. Fluid Mech.*, **222**, 665–691 (1991).
6. T. N. Lyu and I. Mudawar, "Statistical investigation of the relationship between interfacial waviness and sensible heat transfer to a falling liquid film," *Int. J. Heat Mass Transfer*, **34**, 6, 1451–1464 (1991).
7. S. G. Bankoff, "Stability study of liquid flow down a heated inclined plane," *Int. J. Heat Mass Transfer*, **14**, 377–385 (1971).
8. B. Spindler, "Linear stability of liquid films with interfacial phase change," *Int. J. Heat Mass Transfer*, **25**, No. 2, 161–173 (1982).
9. Yu. Ya. Trifonov, "Effect of finite-amplitude waves on evaporation of a liquid film flowing down vertical wall," *Prikl. Mekh. Tekh. Fiz.*, **34**, No. 6, 64–71 (1993).
10. A. Miyara, "Numerical analysis on heat transfer of falling liquid films with interfacial waves," in: *Proc. of the 11th Int. Heat Trans. Conf.* (Kyondju, Korea, Aug. 23–28, 1998), Vol. 2, Korean Soc. Mech. Engineers Seoul (1998), pp. 57–62.
11. A. N. Pavlenko and V. V. Lel', "Heat transfer and crisis phenomena in falling films of cryogenic liquid," *Russ. J. Eng. Thermophys.*, **7**, Nos. 3/4, 177–210 (1997).
12. S. V. Alekseenko, A. D. Nazarov, A. N. Pavlenko, et al., "Flow of a cryogenic liquid film on a vertical surface, *Teplofiz. Aéromekh.*, **4**, No. 3, 307–318 (1997).
13. O. Yu. Tsvelodub, "Solitons on a falling film with low discharge of the liquid," *Prikl. Mekh. Tekh. Fiz.*, No. 3, 64–66 (1980).
14. H. C. Chang, "Onset of nonlinear waves on falling films," *Phys. Fluids A*, **1**, No. 8, 1314–1327 (1989).